JOURNAL OF MATERIALS SCIENCE 33 (1998) 2391–2396

Grain growth in sol–gel derived alumina–zirconia composites

V. V. SRDIĆ, D. I. SAVIĆ
University of Novi Sad, Faculty of Technology, Department of Inorganic Technology and Materials Science, 21000 Novi Sad, Yugoslavia
E-mail: srdicvv@uns.ns.ac.yu

Grain-growth kinetics in sol–gel derived alumina–zirconia composites, containing 20 wt % ZrO_2 stabilized with 0, 3 and 6 mol % ceria have been examined. The growth of alumina grains was effectively retarded by zirconia particles and a lake of abnormal growth was evident. Coupled grain growth was observed, but only if the required minimal sintering conditions (i.e. minimal sintering density) were reached. Measured grain-growth exponents indicate that the grain-boundary diffusion-controlled growth is probably the dominant rate-controlling mechanism in this system. © *1998 Chapman & Hall*

1. Introduction

Zirconia-toughened alumina has become one of the important engineering ceramics, because the room-temperature fracture toughness of alumina can be significantly increased in the presence of dispersed zirconia particles [1–4]. It is also well known [5–9] that a suitable dispersion of zirconia particles in polycrystalline alumina matrix is very effective in inhibiting alumina grain growth and prevents abnormal grain growth. The drag effect of zirconia particles is regarded as the Zener's pinning effect [10]. Zener was the first to predict the limiting grain size, D, as a function of the volume fraction, f, and radius, r, of the second-phase particles

$$\frac{D}{r} = \frac{4}{3f} \tag{1}$$

This relation is often termed the Smith–Zener equation, and means that in dense two-phase systems the grains and particles mutually constrain one another, and the growth of the faster growing phase will be limited by the growth rate of the slower one. In other words, the grain growth is coupled, i.e. both phases coarsen, but only the scale and not the character of the microstructure changes.

The models for grain growth controlled by second-phase particles have commonly suggested [8, 11] that two processes are responsible for the microstructure coarsening: Ostwald ripening and coalescence. Grain-growth kinetics for both processes have been predicted to be governed by a power-law relationship

$$D_t^n - D_0^n = K \tag{2}$$

where D is the grain diameter at time t, D_0 is the initial grain diameter (at $t = 0$), K is the grain-growth constant, and n is the grain-growth exponent. The grain-growth exponent, n, can take different values depending on the dominant flux path [6, 8, 9]. Thus, $n = 3$ for volume-diffusion controlled coarsening and $n = 4$ for boundary-diffusion controlled coarsening. The same power law relationship describes the coupled growth of second-phase particles.

The presented study is concerned with the grain-growth kinetics in the sol–gel derived alumina–zirconia composites. Emphasis is given to the better understanding of microstructural evolution, as this is the key for a successful composite processing.

2. Experimental procedure

The starting alumina–zirconia composites, containing 20 wt % ZrO_2 (on an oxide basis) stabilized with 0, 3 and 6 mol % CeO_2, were obtained by mixing separately prepared aqueous alumina sols, aqueous zirconia sol and aqueous cerium nitrate solution. The details of the preparation were reported elsewhere [12, 13].

Three different aqueous alumina sols, boehmite sols with 5 and 50 wt % α-Al_2O_3 and pure α-Al_2O_3 suspension, were prepared for composites with notation 3_k-A_c, 3_k-AC and 3_k-C, respectively (where k denotes the ceria content). These sols were produced by ultrasonically dispersing high-purity boehmite powder ($> 99.99\%$, boehmite powder H-3500, Advanced Ceramic Corp., OH, USA) and/or α-alumina powder ($> 99.97\%$ Ceralox HPA 0.5, average particle size 0.25 μm, Condea Chemie, Germany) in distilled water with nitric acid at pH $\approx$ 2.5 and at room temperature. The small portion of α-Al_2O_3 was added only to seed the boehmite sol, but larger portions of α-Al_2O_3 were also added to increase the solid concentration at the gel point and reduce the cracking during drying [12].

The zirconia sol was prepared by hydrolysis of zirconium-*n*-propoxide (Zr^nPr, Fluka Chemie, CH), dissolved in anhydrous ethanol (0.6 mol Zr^nPr/litre)

TABLE I Notation and composition of alumina–zirconia composites

Sample notation	Amount of precursors (on the oxide basis) (wt %)			Ceria content in ZrO_2 (mol %)
	AlOOH	α-Al_2O_3	$ZrO_2 + CeO_2$	
3_0-A_c	0.76	0.04	0.2	0
3_0-AC	0.4	0.4	0.2	0
3_3-AC	0.4	0.4	0.2	3.0
3_6-AC	0.4	0.4	0.2	6.0
3_0-C	–	0.8	0.2	0
3_3-C	–	0.8	0.2	3.0
3_6-C	–	0.8	0.2	6.0

with distilled water under acidic conditions (pH $\approx$ 1) and at room temperature (alkoxide, water and nitric acid molar ratio was 1 : 2 : 0.5), and then by continuous evaporation and replacing the ethanol with distilled water without changing the concentration and pH.

Aqueous cerium nitrate ($Ce(NO_3)_3 \cdot 6H_2O$, The British Drug Houses Ltd, UK) solution, containing 0.2 mol $Ce(NO_3)_3$/litre, was used as the source of ceria.

Appropriate portions of the alumina sols, the zirconia sol and the cerium nitrate solution were mixed together (Table I). Ultrasonically mixed composite sols were gelled by slow evaporation at 70 °C and then carefully dried in air for a few days. Dried gel fragments (up to a few centimetres) were heat treated in air at 600 °C/1h, 1100 °C/1h and 1500 °C/1h at 10 °C/min^{-1}, and finally sintered at 1550 °C for 20, 60, 120, 300 and 600 min.

The bulk density of the sintered samples was measured by Archimedes' method (the porous samples were coated with paraffin). The relative densities of the alumina–zirconia composites were calculated using the theoretical values 5.8 g cm^{-3} for m-ZrO_2, 6.1 g cm^{-3} for t-ZrO_2 and 3.98 g cm^{-3} for α-Al_2O_3. The portions of tetragonal and monoclinic zirconia were determined using the integrated intensity of the tetragonal (1 1 1) and two monoclinic (1 1 1) and (1 1 $\bar{1}$) peaks [14]. The microstructure of the polished and thermally etched surfaces were examined using a scanning electron microscope (SEM Jeol – JSM35). Grain size was determined by the linear intercept method [15] on more than 300 grains for each sample.

3. Results and discussion

The relative densities of the alumina–zirconia composites versus sintering time at 1550 °C are presented in Fig. 1. The 3_0-A_c composite, seeded with 5 wt % α-Al_2O_3 particles, has a relatively high starting density (the density of composite sintered at 1500 °C for 60 min), that increases mildly with isothermal sintering (Fig. 1a). The starting densities of the other two unstabilized composites with a higher portion of α-Al_2O_3 particles in the original sol (3_0-AC and 3_0-C) are considerably lower, but the increase with sintering time is more pronounced. The relative density decreases not only with increasing portion of α-Al_2O_3 in the original sol, but also with increasing ceria content (Fig. 1b and c). The effect of ceria on the sintering process originates from the considerable influence of cerium nitrate on the gelation of alumina–zirconia sols. As already reported [12], cerium nitrate accelerates aggregation of the nanosized (alkoxide-derived) zirconia particles during the composite sol formation and sol/gel transition, producing less homogeneous composite gel microstructures with lower density.

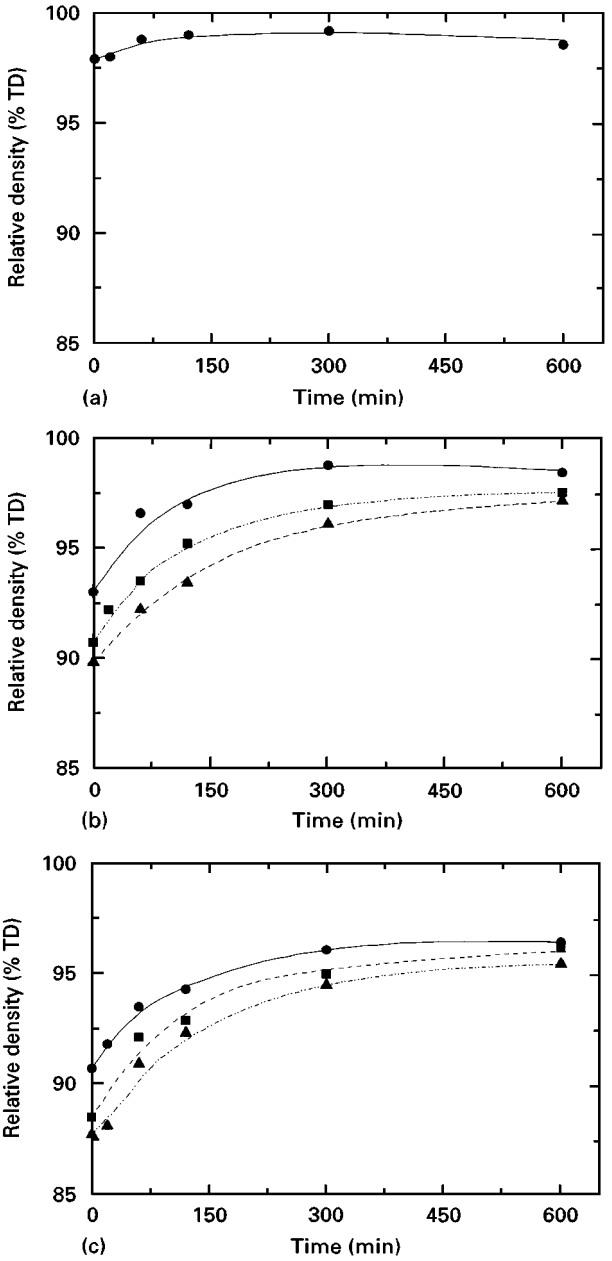

Figure 1 Change in relative density of (a) 3_0-A_c, (b) (●) 3_0-AC, (■) 3_3-AC, (▲) 3_6-AC, and (c) (●) 3_0-C, (■) 3_3-C, (▲) 3_6-C composites against sintering time at 1550 °C.

Microstructure coarsening at 1550 °C is shown in Fig. 2 for the 3_0-A_c, 3_0-AC and 3_0-C composites. The dark and bright contrasts in the scanning electron micrographs are alumina grains and zirconia particles, respectively. In all the composites, a lake of abnormal alumina grain growth during isothermal sintering is evident. Zirconia particles are well-distributed and are primarily located at alumina grain junctions, whereas only a small portion can be seen at the grain edges.

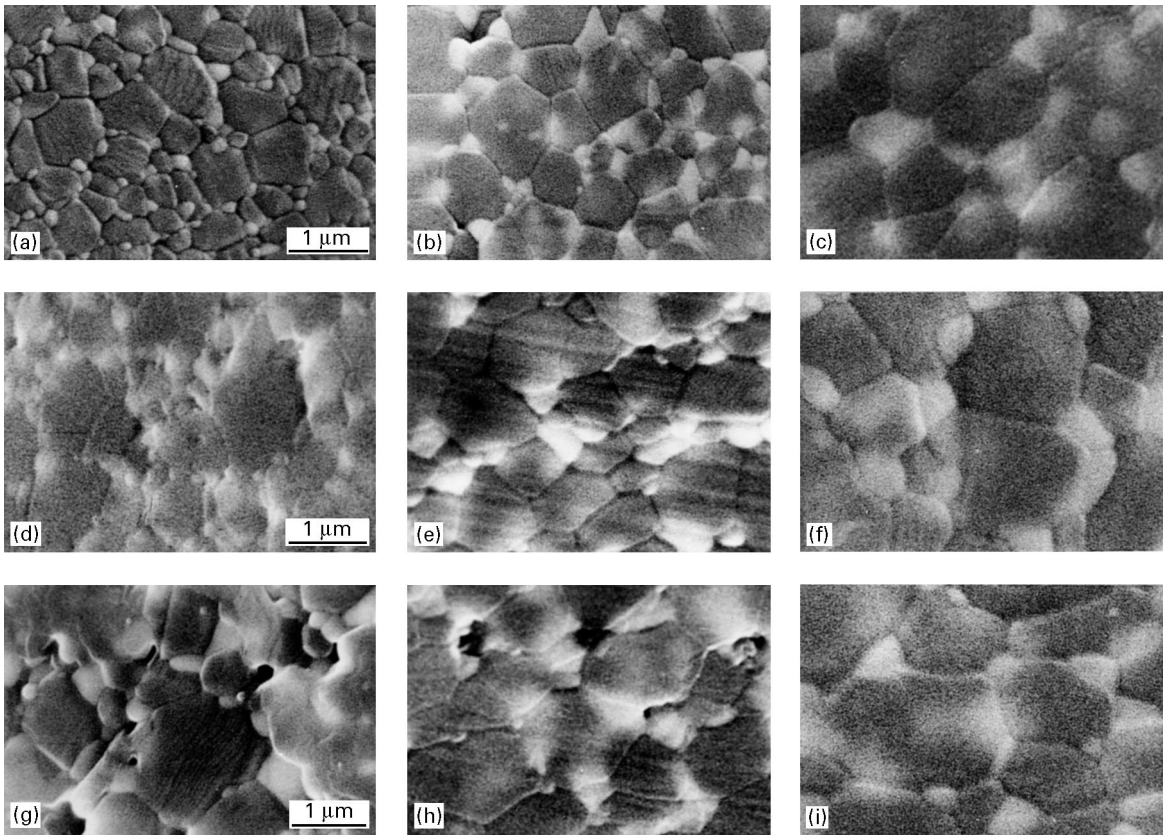

Figure 2 Scanning electron micrographs of the 1500 °C sintered alumina–zirconia composites: 3_0-A_c: (a) 1500 °C 1 h, (b) 1500 °C 2 h, (c) 1550 °C 10 h; 3_0-AC: (d) 1500 °C 1 h, (e) 1550 °C 2 h, (f) 1550 °C 10 h; 3_0-C: (g) 1500 °C 1 h, (h) 1550 °C 2 h, (i) 10 h.

The composites, with a higher portion of α-Al_2O_3 in the original sol (3_0-AC and 3_0-C), have somewhat coarser and less homogeneous microstructures and a higher degree of porosity. Notably, although zirconia is the slower growing phase in the alumina/zirconia system, it seems that in these two composites the growth of zirconia particles is faster than the growth of alumina grains (Fig. 2).

The change in mean size of alumina grains and zirconia particles in the unstabilized alumina–zirconia composites (3_0-A_c, 3_0-AC and 3_0-C) with time at 1550 °C is shown in Fig. 3a. Grain size increases with each increment of sintering time. The growth behaviour of zirconia particles is similar in all samples, but the difference in initial alumina grain growth is obvious. The faster initial growth of alumina grains exhibit the 3_0-A_c composite. Fig. 3b shows the comparison of grain-growth behaviour for the alumina-zirconia composites with difference ceria contents (3_0-AC, 3_3-AC and 3_6-AC). No considerable differences can be observed either for alumina or for zirconia.

The ratio of mean alumina grain size, D, to mean zirconia particle radius, r, is plotted against sintering time in Fig. 4. The D/r ratio remains almost constant during all sintering times at 1550 °C for the 3_0-A_c composites. This is in agreement with Smith–Zener's model [10], but the D/r ratio of about 5.4 measured in the presented study (Fig. 4), confirmed the observed disagreement with this model [7, 16, 17], that overestimates the predicted net restraining force caused by second-phase (zirconia) particles. However, for all other composite samples, the D/r ratio reaches the constant values (of about 5.4) just after the initial decreases during the initial sintering period. This can be explained by uncontrolled growth of alumina grains during the presintering treatment, probably due to insufficient efficiency of the distributed zirconia particles. The poor efficiency of zirconia particles in these composites, as compared to the 3_0-A_c one, is ascribed to less homogeneous composite microstructures caused by the presence of a high portion of the large original α-alumina particles and the already mentioned ceria effect [12]. Thus, during microstructural coarsening, a point where the driving force for boundary migration is balanced by the drag force of the zirconia particles is reached just at certain sintering conditions. Because this moment is characterized by very large alumina grains in comparison with the zirconia particles (Figs 2d and g), the coupled grain growth begins just after establishing the equilibrium D/r ratio for the corresponding volume fraction of zirconia (Fig. 4). It seems (Fig. 4) that a longer sintering time is needed to attain the point with constant D/r ratio in composites with lower densities, confirming that the minimal sintering conditions (i.e. minimal composite density) are required for coupled grain growth.

Grain-growth kinetics was examined with log–log plots of $(D_t^n - D_0^n)$ versus sintering time (Fig. 5). The grain sizes of the composites sintered at 1500 °C for 60 min are used as the D_0 values, and the integer values 3 and 4 for the grain-growth exponents n. For

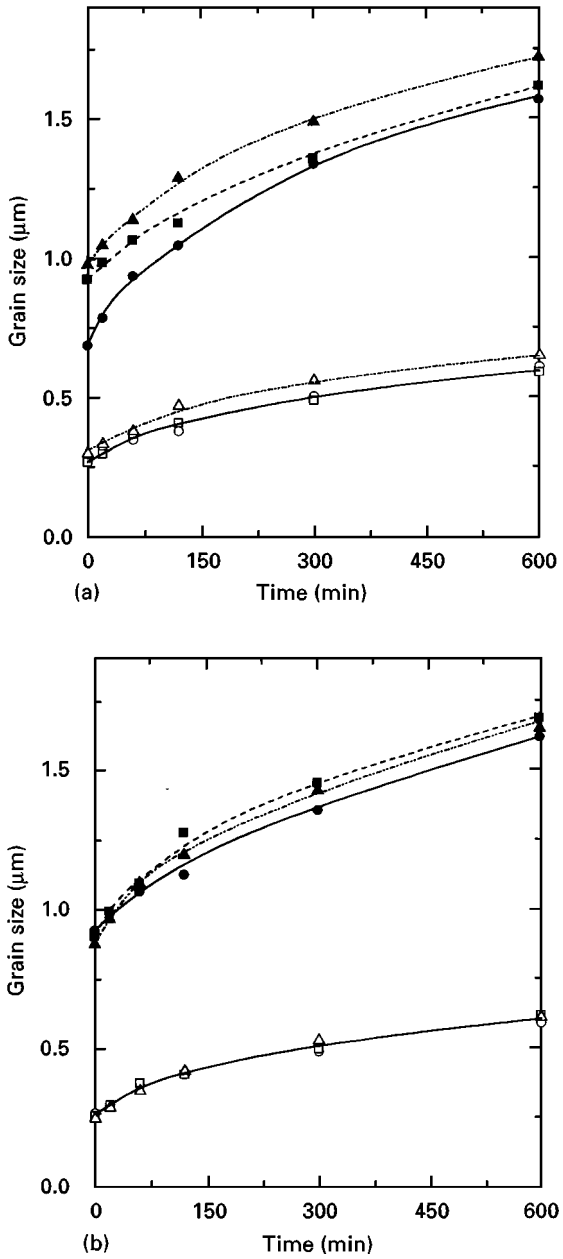

Figure 3 Mean (●, ■, ▲) alumina grain and (○, □, △) zirconia particle sizes as a function of sintering time at 1550 °C: (●, ○) 3_0-A_c, (a) (■, □) 3_0-AC, (▲, △) 3_0-C; (b) (■, □) 3_3-AC, (▲, △) 3_6-A_c.

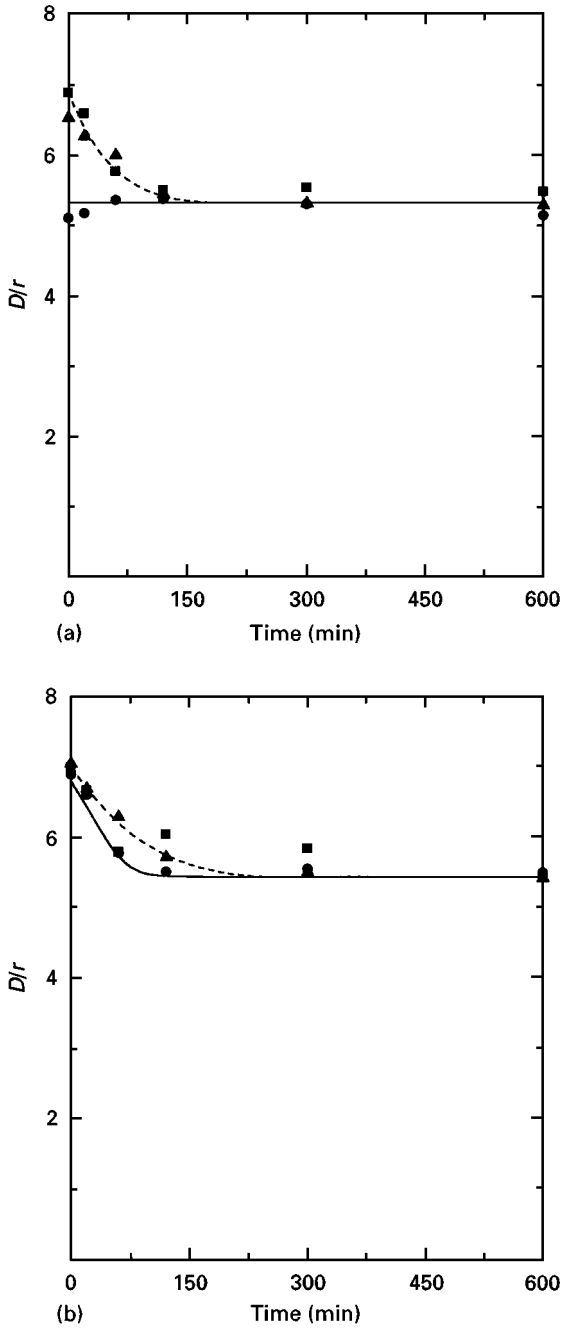

Figure 4 Effect of sintering time at 1550 °C on the ratio of mean alumina grain size to mean zirconia particle radius (D/r). (a) (●) 3_0-A_c, (■) 3_0-AC, (▲) 3_0-C. (b) (●) 3_0-AC, (■) 3_3-AC, (▲) 3_6-AC.

the correct grain-size exponent n, the log–log plots should have a slope of 1. It is clear from Fig. 5 that all the zirconia plots and the alumina plot for 3_0-A_c sample based on n values between 3 and 4, yield slopes which closely approximate unity, but other alumina plots have a slope of 1 for grain-growth exponent larger than 4. The calculated values of the grain-growth exponents are shown in Table II. The grain-growth exponents of alumina, n_a, and zirconia, n_z, have similar values only for the 3_0-A_c composites, indicating the coupled grain growth for all examined sintering times. The observed grain-growth exponents $n_a = 3.7$ and $n_z = 3.4$ for the 3_0-A_c composite are somewhat lower than those reported by Hori *et al.* [18] and Okada and Sakuma [9]. The reason could be their assumption that D_0 is negligible, which would increase the measured grain-growth exponent [8]. Assuming that the activation energies in different alumina–zirconia systems indicate sintering controlled by grain-boundary diffusion [8, 9, 19], it can be concluded that the measured grain-growth exponents for the 3_0-A_c composite are in good agreement with the prediction that the grain-boundary diffusion-controlled growth is the dominant rate-controlling mechanism in this system.

Unlike the 3_0-A_c composite, the considerable difference between n_a and n_z is evident in all other composites (Table II), indicating the different growth kinetics of alumina and zirconia phases. Because the zirconia grain-growth exponents have similar values, the same growth mechanism of zirconia particles in these and the 3_0-A_c composites is predicted. However,

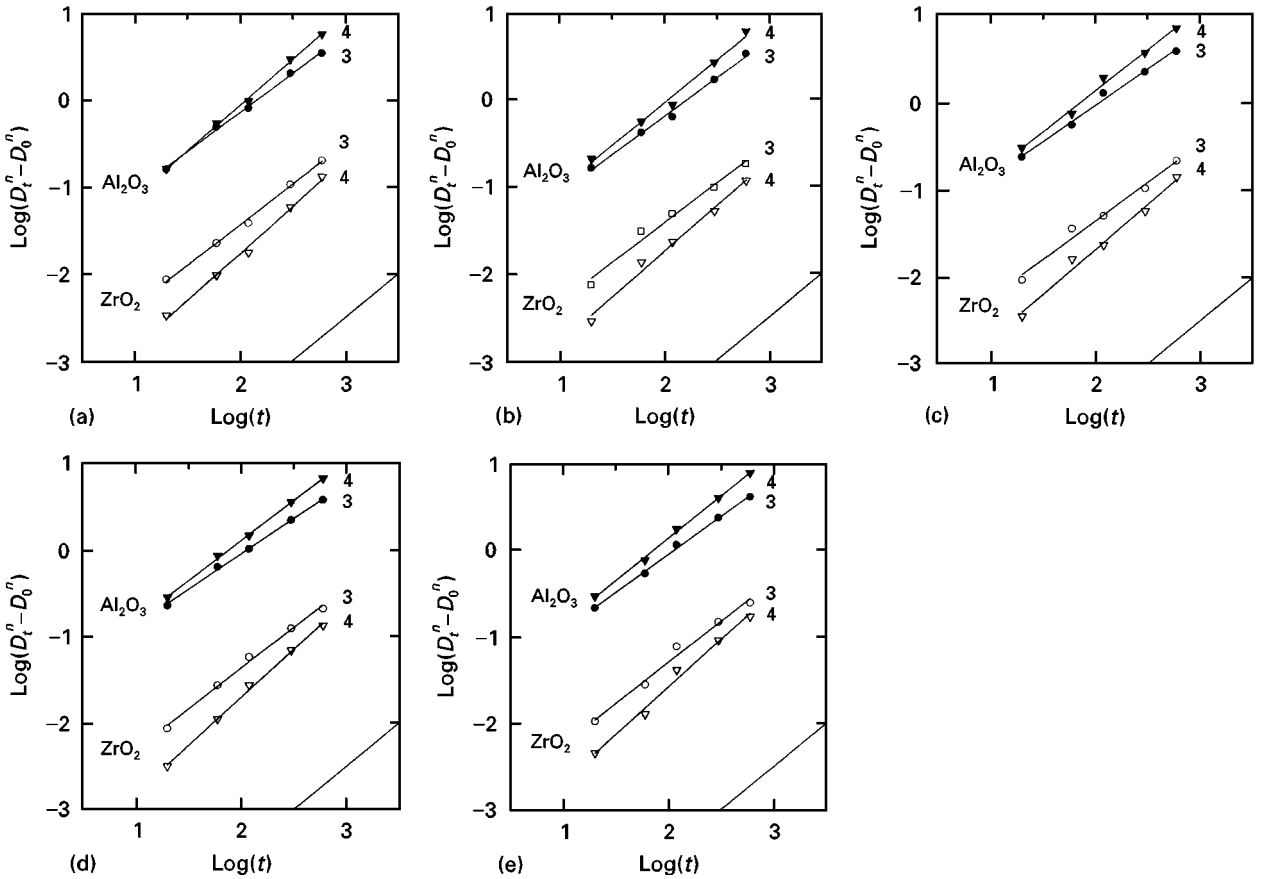

Figure 5 The log $(D_t^n - D_0^n)$ versus log(t) for two integer values of grain-growth exponent: $n = 3$ and 4. The correct slope equal to 1 is indicated by the line in the right-hand corner of each figure. (a) 3_0-A_c, (b) 3_0-AC, (c) 3_3-AC, (d) 3_6-AC, (e) 3_0-C.

TABLE II Alumina and zirconia grain-growth exponents, n

Sample notation	n, Al_2O_3	n, ZrO_2
3_0-A_c	3.7	3.4
3_0-AC	4.2	3.6
3_3-AC	4.5	3.8
3_6-AC	4.6	3.4
3_0-C	4.2	3.3

the larger alumina grain-growth exponents ($n_a > 4$) confirmed the already mentioned uncontrolled growth of the alumina grains during the initial sintering period. A decreasing tendency of n_a is observed, when the grain sizes of the samples with higher densities (sintered at 1550 °C for 20 or 60 min) are used as the D_0 values.

4. Conclusion

Grain-growth kinetics in sol–gel derived alumina–zirconia composites, containing 20 wt % ZrO_2 stabilized with 0, 3 and 6 mol % CeO_2, at 1550 °C has been examined. Coupled grain growth throughout all the sintering experiments is observed only in a fully dense composite. However, for composites with lower densities, the ratio of mean alumina grain size to mean zirconia particle size reaches a constant value just after the initial decrease during the initial sintering period, indicating that minimal sintering conditions are required for coupled grain growth. The observed grain-growth exponents around 3.5–4 indicate that the grain-boundary diffusion-controlled growth is the dominant rate-controlling mechanism in the alumina–zirconia system. It is also shown that ceria has no considerable effect on the grain-growth behaviour.

References

1. N. CLAUSSEN, *J. Am. Ceram. Soc.* **59** (1976) 49.
2. J. WANG and R. STEVENS, *J. Mater. Sci.* **24** (1989) 3421.
3. A. BLEIER, P. F. BECHER, K. B. ALEXANDER and C. G. WESTMORELAND, *J. Am. Ceram. Soc.* **75** (1992) 2649.
4. V. V. SRDIĆ and L. RADONJIĆ, *J. Am. Ceram. Soc.* **80** (1997) 2056.
5. F. F. LANGE and M. M. HIRLINGER, *ibid.* **67** (1984) 164.
6. B. W. KIBBEL and A. H. HEUER, in "Advances in Ceramics", Vol. 12, "Science and Technology of Zirconia II", edited by N. Claussen, M. Ruhle and A. H. Heuer (American Ceramic Society, Columbus, OH, 1984) p. 415.
7. K. OKADA and T. SAKUMA, *J. Ceram. Soc. Jpn* **100** (1992) 382.
8. K. B. ALEXANDER, P. F. BECHER, S. B. WATERS and A. BLEIER, *J. Am. Ceram. Soc.* **77** (1994) 939.
9. K. OKADA and T. SAKUMA, *Br. Ceram. Trans.* **93** (1994) 71.
10. C. ZENER, private communication referenced by C. S. SMITH, *Trans. AIME* **175** (1948) 15.
11. G. T. HIGGINS, S. WIRYOLUKITO and P. NASH, *Mater. Sci. Forum* **94–95** (1992) 671.
12. V. V. SRDIĆ and L. RADONJIĆ, in "Engineering Ceramics' 96", '*Higher Reliability through Processing*' edited by G. N. Babini, M. Haviar and P. Šajgalik (Kluwer Academic, The Netherlands, 1997) p. 61.

13. V. V. SRDIĆ and L. RADONJIĆ, *Ceram. Int.* **21** (1995) 5.
14. H. TORAYA, M. YOSHIMURA and S. SOMIYA, *J. Am. Ceram. Soc.* **67** (1984) C-119.
15. J. C. WURST and J. A. NELSON, *ibid.* **55** (1972) 109.
16. Y. LUI and B. R. PATTERSON, *Scripta Metall. Mater.* **27** (1992) 539.
17. M. HILLERT, *Acta Metall.* **36** (1988) 3177.
18. S. HORI, R. KURITA, M. YOSHIMURA and S. SOMIYA, *J. Mater. Sci. Lett.* **4** (1985) 1067.
19. J. WANG and R. RAJ, *J. Am. Ceram. Soc.* **74** (1991) 1959.

Received 31 January 1997
and accepted 27 January 1998